Nuclear Instruments and Methods in Physics Research B 269 (2011) 894–900

Contents lists available at ScienceDirect

Nuclear Instruments and Methods in Physics Research B

journal homepage: www.elsevier.com/locate/nimb

Nanoscale pattern formation at surfaces under ion-beam sputtering: A perspective from continuum models

Rodolfo Cuerno [a,*], Mario Castro [b], Javier Muñoz-García [c], Raúl Gago [d], Luis Vázquez [d]

[a] Departamento de Matemáticas and Grupo Interdisciplinar de Sistemas Complejos (GISC), Universidad Carlos III de Madrid, Avenida de la Universidad 30, E-28911 Leganés, Madrid, Spain
[b] GISC and Grupo de Dinámica No Lineal (DNL), Escuela Técnica Superior de Ingeniería (ICAI), Universidad Pontificia Comillas, E-28015 Madrid, Spain
[c] Systems Biology Ireland and GISC, University College Dublin, Belfield, Dublin 4, Ireland
[d] Instituto de Ciencia de Materiales de Madrid, Consejo Superior de Investigaciones Científicas, E-28049 Madrid, Spain

ARTICLE INFO

Article history:
Received 30 July 2010
Received in revised form 7 November 2010
Available online 30 November 2010

Keywords:
Nanoscale pattern formation
Ion-beam sputtering
Surfaces
Morphological instabilities
Continuum models

ABSTRACT

Although reports on surface nanostructuring of solid targets by low to medium energy ion irradiation date back to the 1960s, only with the advent of high resolution tools for surface/interface characterization has the high potential of this procedure been recognized as a method for efficient production of surface patterns. Such morphologies are made up of periodic arrangements of nanometric sized features, like ripples and dots, with interest for technological applications due to their electronic, magnetic, and optical properties. Thus, roughly for the last ten years large efforts have been directed towards harnessing this nanofabrication technique. However, and particularly in view of recent experimental developments, we can say that the basic mechanisms controlling these pattern formation processes remain poorly understood. The lack of nanostructuring at low angles of incidence on some pure monoelemental targets, the role of impurities in the surface dynamics and other recent observations are challenging the classic view on the phenomenon as the mere interplay between the curvature dependence of the sputtering yield and surface diffusion. We review the main attempts at a theoretical (continuum) description of these systems, with emphasis on recent developments. Strong hints already exist that the nature of the morphological instability has to be rethought as originating in the material flow that is induced by the ion beam.

1. Introduction

Observations of nano-scale patterns on the surfaces of solid targets that undergo irradiation by 100 eV to 10 keV ions, date back at least to the early 1960's [1,2]. They correspond to materials that either are amorphous like glass, or become amorphized by this type of bombardment like monocrystalline semiconductors such as Si [3]. These are the type of targets that we will be considering in the present work. Actually, quite similar patterns are found on other materials, such as metallic [4] or insulating targets, see e.g. [5,6] for reviews, but additional physical effects are expected to come into play into their pattern forming properties.

Already in the first accounts of these shapes, and due to the naked eye similarities, natural analogies were drawn to more familiar patterns, like ripples that form in a self-organized fashion on the surface of sandy dunes, due to the action of wind or water. Examples illustrating these analogies can be found in Fig. 1. As it turns out, this analogy has played a fruitful role in the modeling of the nanostructures formed by ion-beam sputtering (IBS), and is expected to maintain as an inspiration for future developments, as seen below.

With the advent of high resolution surface characterization techniques, important geometrical features of these structures were revealed, such as the large degree of in-plane ordering that they can develop [7], which is of clear practical importance to applications ranging from optoelectronic to catalytic. Moreover, the universality of their production has been assessed [6], in the sense of the high degree of independence on the specific ion-target combination, as well as the dependence of their shape (e.g. rippled vs dot-like) only on rather general geometrical constraints, such as the symmetry of the experimental set-up (ripples for oblique angles of incidence $\theta \neq 0$ and dots for normal incidence $\theta = 0$, or else for oblique incidence onto a rotating target), although some exceptions to these rules can be found, see e.g. [8]. From the point of view of understanding the physical processes that govern this pattern formation phenomenon, a crucial input concerns the availability of data on the time evolution of these systems. At this, one has to take into account the range of fluxes that is usually employed, typically 1 to 10 ion nm^{-2} s^{-1}. Thus, the time scale associated with

* Corresponding author. Tel.: +34 91 6245944; fax: +34 91 6249129.
E-mail address: cuerno@math.uc3m.es (R. Cuerno).

0168-583X/$ - see front matter © 2010 Elsevier B.V. All rights reserved.
doi:10.1016/j.nimb.2010.11.072

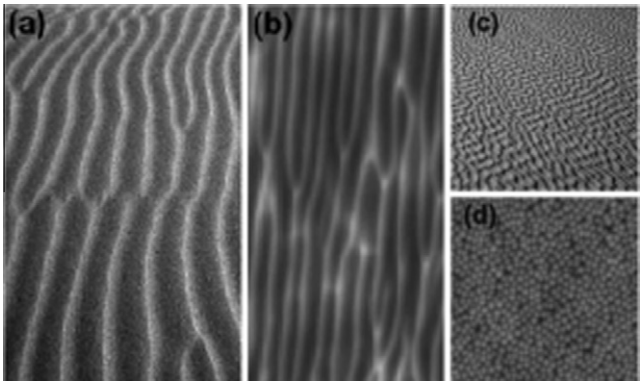

Fig. 1. From Ref. [6], by permission: (a) ripples on a sand dune in Morocco, courtesy of J. Rodríguez and E. Blesa. (b) 3.7 μm^2 top view AFM image of a Si surface immersed in argon plasma. (c) "Dots" on a sand dune. Copyright Bruce Molnia, Terra Photographics. Image Courtesy Earth Science World Image Bank http://www.earthscienceworld.org/images. (d) 1 μm^2 top view AFM image of a GaSb surface irradiated by 0.7 keV Ar^+ ions under normal incidence.

ion beam nanostructuring ($\simeq$1 s) is orders of magnitude slower than the typical times ($\simeq$1 ps) associated with the relaxation of collision cascades or with surface diffusion hopping attempts. This induces the occurrence of non-trivial changes in the morphological evolution at macroscopic time scales (from seconds to hours).

Coming back to the analogy with macroscopic patterns, it is instructive to compare typical magnitudes both in IBS nano-patterned systems and, e.g., ripple formation on aeolian sand dunes. Thus, ripple formation and coarsening has been observed for off-normal Ga^+ bombardment of Si at 30 keV [9]. The ripple wavelength at instability onset was near 50 nm, ripples being transported in-plane with a velocity close to 0.3 nm/s. Quite similar figures were obtained more recently for off-normal irradiation of glass with similar beam characteristics [10]. Meanwhile, field and laboratory experiments on the formation of aeolian ripples indicate typical wavelengths around 6 cm and ripple transport speeds at 0.07 cm/s [11]. Hence, while there is a difference of 6 orders of magnitude in length scales, the typical times needed to travel the corresponding wave-length distances are both of the order of seconds. We conclude that IBS nanopatterning is quite a slow phenomenon (incidentally, $0.3\ \mathrm{nm\,s^{-1}} \simeq 1\ \mathrm{cm\,year^{-1}}$ is a typical speed for tectonic plate motion!).

As time scales of the order of seconds remain beyond reach for microscopic or atomistic approaches like Molecular-Dynamics (MD) or even kinetic Monte Carlo [12,13], continuum descriptions appear as a natural choice in order to account for the main properties of these pattern forming systems. The universality of the phenomena in the sense of their occurrence for a wide choice of ion-target combinations and incidence geometries adds credit to the applicability of this type of models. During the last twenty years or so, we have witnessed the application of continuum descriptions to IBS nanopatterns with a varying (and in general increasing) degree of success. However, a number of quite recent experimental observations are forcing us to rethink this modeling from a new perspective. It is the purpose of this work to overview the main steps taken in the process as well as to point out potential new avenues for this thriving activity.

2. Bradley–Harper-type models

Historically, the work that paved the way for further continuum modeling of IBS surface nanopatterns is due to Bradley and Harper (BH) [14]. The procedure amounts to assuming that collision cascades relax infinitely fast so that one can compute the local velocity of erosion at a surface point on the target as proportional to the total energy that is thus deposited in its surroundings. It had been already pointed out by Sigmund [15] that this assumption leads to what is known as a morphological instability: due to this mechanism, the bottom of a trough is eroded faster than a surface peak, so that initial height inhomogeneities will be amplified. Using Sigmund's Gaussian description for energy deposition within the linear cascade regime [15], BH then performed a small slope approximation that allowed them to obtain a closed evolution equation for the target surface height $h(\mathbf{r},t)$ as (we provide the main terms, after appropriate choice of a reference frame) [14]

$$\frac{\partial h}{\partial t} = -v_x \partial_x^2 h - v_y \partial_y^2 h - B\nabla^4 h, \tag{1}$$

where coefficients $v_{x,y}$ depend on phenomenological parameters like flux, average ion energy, average penetration depth, and other features of the chosen distribution for energy deposition. Some comments on Eq. (1) are in order. First, in BH's original derivation the third term on the rhs was put forward *ad-hoc* in order to introduce an smoothing mechanism that controls the small scale behavior of the system. Physically, their choice corresponds to thermal surface diffusion as classically described by Mullins [16]. Note that in such a case the coefficient B becomes proportional to parameters such as the surface diffusivity coefficient, that only depends on temperature in Mullins' derivation. However, irradiation is expected to influence the value of the latter property [17], the present approach being incapable of reflecting this fact. Second, the BH equation, albeit successful in explaining a number of experimental observations including the ripple orientation with respect to the ion beam (see a review in [5]), cannot be a complete description of the process, as it predicts exponential blow-up of the surface height.

Natural improvements of the BH framework were subsequently attempted [18,19], see [20] for a unified presentation. The most salient features of these were non-linear effects that are able to tame the BH instability and drive the surface to a stationary state, and contributions to the equation of motion that take the shape of surface diffusion terms, but with a purely erosive origin unrelated to actual material transport. Technically, these terms originate in the description of the surface geometry to a high order of approximation. Considering the case of normal incidence for simplicity, the ensuing interface equation takes the following shape

$$\frac{\partial h}{\partial t} = -\nu\nabla^2 h - \mathscr{K}\nabla^4 h + \lambda(\nabla h)^2 + \eta, \tag{2}$$

where $\mathscr{K} = B + D$ collects the erosive contribution to the surface diffusion term, D, together with the previous Mullins'-type one, B. In principle, in Eq. (2) a noise term η is allowed to account for fluctuations in the ion-beam flux, although the large scale fluctuations that this equation develops render stochastic contributions of a secondary importance. Like in BH's derivation, all the coefficients in Eq. (2) are derived as functions of parameters characterizing the erosion system, leading to an improved description that, beyond dynamical saturation of the ripple amplitude, also provided an explanation for dependence of pattern characteristics with parameters such as ion energy and flux, and temperature in appropriate condition ranges [20].

In the context of Non-linear Science, Eq. (2) is known as the (stochastic) Kuramoto–Sivashinsky (KS) equation, and is a paradigm for chaotic spatially extended systems [21]. The anisotropic versions of it derived in [18–20] thus become anisotropic generalizations of the KS equation. Summarizing a behavior that can be quite rich in its mathematical structure, to our purposes the main features of the dynamics described by the KS equation consist in an initial (BH) morphological instability in which a preferred (dot or ripple) wavelength is selected. This regime corresponds to fast (exponential) growth of e.g. the surface roughness. After this

transient time, the surface amplitude stabilizes, entering a second regime in which the pattern evolves in a highly nonlinear fashion becoming disordered both in plane and in the growth direction, with fluctuations that display kinetic roughening properties [22]. This type of behavior applies to the observed evolution of some IBS nanopatterns [23], but the generically expected and technologically appealing case in which well ordered dots or ripples form, remains far from description by the KS equation proper. Thus, for a number of years various attempts were made at improved descriptions through further generalizations of the KS equation. We can mention the damped KS equation in which a linear term of the form $-\kappa h$ is added to the rhs of Eq. (2) [24]. This additional term is well known in the Pattern Formation context to allow for improved ordering of the cellular structure (dots) for appropriate parameter conditions. However, to date, there is not a satisfactory physical interpretation of the damping parameter κ. Another possibility to go beyond the KS equation is to carry out the BH-type expansion to still a higher non-linear order, as indeed was done in [25], obtaining an interface equation that for normal incidence reads

$$\frac{\partial h}{\partial t} = -\nu\nabla^2 h - \mathscr{K}\nabla^4 h + \lambda^{(1)}(\nabla h)^2 + \lambda^{(2)}\nabla^2(\nabla h)^2. \tag{3}$$

Unfortunately, coefficients $\lambda^{(1,2)}$ take the same sign as functions of phenomenological parameters, so that there may be a cancellation mode in Eq. (3) [26,27]. This means that the wave-vector value $k = (\lambda^{(1)}/\lambda^{(2)})^{1/2}$ is linearly unstable and that nonlinear terms may exactly cancel each other for its equation of motion, so that its amplitude blows up exponentially, as a result of which the continuum description breaks down. In summary, the BH approach based on the *ad-hoc* combination of the erosion rate and surface diffusion effects not only may be of a limited physical applicability, but is also affected by issues on mathematical consistency. Note that probably this is not necessarily due to employing Sigmund's Gaussian description of energy deposition: as seen for exponential [28] as well as for more general [29] energy deposition functions, the main qualitative pattern-forming properties are essentially unchanged as compared with those induced by Gaussian decay.

3. Two-field "hydrodynamic" models

Having reached this point in the continuum description of IBS induced nanopatterns, by 2005 there was a need for an improved continuum model that: (i) introduced an increased number and type of relaxation mechanisms in a natural (non *ad-hoc*) way that allows for an interaction among them and for the expected interplay between transport and morphology; (ii) improves upon consistency issues (cancellation modes, etc.); (iii) can in principle be adapted to improvements in the description of energy distribution; (iv) can account for the main physical phenomena above within an unified framework, conspicuously including in-plane order and coarsening properties of the pattern, and (v) generalizes previous linear and non-linear models, incorporating their successes and improving upon their shortcomings. In order to implement this research program, a timely observation by Aste and Valbusa [30] brought back attention to the analogy with macroscopic pattern formation noted in Section 1. The idea is that for aeolian or underwater sand ripples, a successful approach is available (see [31] for a review) in which the surface dynamics is coupled with that of the density of species whose transport gives rise to the physical correlations across the sand dune, that will eventually lead to the pattern formation process. Thus, one needs to describe in more detail the near-surface region in order to properly account the system dynamics.

Actually, the formation on semiconductors of a thin amorphous layer on top of a crystalline bulk under the present type of irradiation is well documented [3]. Typical figures as assessed e.g. by MD indicate [32] a stationary thickness of 2–3 nm for 500 eV Ar^+ irradiation of Si, that is readily produced for a fluence of $4 \cdot 10^{14}$ ions cm^{-2}. With a sputtering yield that stabilizes at around 0.45 under the previous irradiation conditions, this implies that, during the morphologically non-trivial evolution, the main effect of the beam is amorphizing the solid while maintaining a stationary amorphous layer, rather than sputtering proper. To some extent one can speak about "local redeposition" in the sense that atoms that are eroded from the crystalline bulk remain ("redeposit back") at the surface, provided the amorphous layer is thin so that it can be loosely identified with the surface itself. Actually, the idea of a thin surface layer that is subject to ion-induced viscous flow had allowed Umbach et al. [33] to improve their description of the temperature dependence of the ripple wavelength for experiments on irradiation of silica.

Capitalizing on these ideas, we have developed this "hydrodynamic" approach for the cases of normal [34] and of oblique incidence [35]. Incidentally, the quotes are in order since this is not yet a full implementation of, say, the Navier–Stokes equations for these systems (see Section 6). We are, rather, borrowing the terminology from the Granular Matter community, wherein this type of continuum approach is dubbed in the present form. In general, we consider a coupled system of equations for the dynamics of the surface height h and of the density of species, R, that are subject to (diffusive) transport within the amorphous layer,

$$\partial_t h = -\Gamma_{ex} + \Gamma_{ad}, \tag{4}$$

$$\partial_t R = (1-\phi)\Gamma_{ex} - \Gamma_{ad} + D\nabla^2 R. \tag{5}$$

Here $\Gamma_{ex}(\Gamma_{ad})$ are rates of excavation (addition) from (to) the crystalline bulk. The idea is that removal of material decreases the value of h and increases that of R, and it is the latter that is transported with diffusivity D. The parameter ϕ controls the amount of local redeposition, as easily seen by its limiting cases. Thus, for $\phi = 1$ all excavated material is immediately sputtered away without contribution to local redeposition, while $\phi = 0$ implies full material conservation. While (4) and (5) are a statement on conservation of matter, proper constitutive laws are required that relate the rates Γ to the physical fields, h and R themselves. A natural choice for Γ_{ex} is [34,35]

$$\Gamma_{ex} = \alpha_0\left[1 + \nabla\cdot(\underline{\alpha_2}\nabla h) + \nabla h\cdot(\underline{\alpha_6}\nabla h) + \cdots\right], \tag{6}$$

where $\underline{\alpha_i}$ are tensors in the general anisotropic case, and one can essentially recognize the rhs of the BH-type statements on the local erosion velocity (1) and (2). Here the scale is fixed by the erosion rate of a flat interface, $\alpha_0 = JY_0\Omega$, that takes typical values in the $0.1–10^4$ nm s^{-1} range, where J is the ion flux, Y_0 is the sputtering yield, and Ω is the atomic volume. On the other hand, the addition rate is chosen so as to reproduce Mullins' surface diffusion in the absence of irradiation (i.e. for $\alpha_0 = 0$), favoring transport from low to high coordination surface sites, in a way that is moderated by curvature, thus (assuming again isotropy in the (x,y) plane in order to simplify the presentation)

$$\Gamma_{ad} = \gamma_0\left[R - R_{eq}(1-\gamma\nabla^2 h)\right]. \tag{7}$$

Here R_{eq} is an "equilibrium" density of mobile species that can be non-zero even in the absence of a beam, γ is surface tension, and $\gamma_0 \simeq 10^9$ s^{-1} sets the time scale associated with e.g. surface diffusion hopping attempts. One indication that system (4) through (7) is a natural continuum description of the present nanoscale phenomena is the fact that it reduces exactly to Mullins' formulation of surface diffusion for $\alpha_0 = 0$, see the second reference in [35].

Although one can study the dynamics of the full set (4) and (5), advantage can be taken from the physical fact that $\epsilon = \alpha_0/(\gamma_0 R_{eq}) \simeq 10^{-10}$–$10^{-5}$ is a non-dimensional small parameter for the situations of interest. This implies that the R field evolves in a much shorter time scale than the height so that power expansion in ϵ leads to a single equation for the latter that reads (for normal incidence $\theta = 0$) [34]

$$\frac{\partial h}{\partial t} = -\nu\nabla^2 h - \mathscr{K}\nabla^4 h + \lambda^{(1)}(\nabla h)^2 - \lambda^{(2)}\nabla^2(\nabla h)^2. \quad (8)$$

Note that this equation has the exact same shape as Eq. (3), but thanks to the sign of its last term on the rhs can become free of cancellation modes. As in previous models, coefficients appearing in Eq. (8) are also (different) functions of phenomenological parameters, and actually couple the various concurrent mechanisms in a natural way. For instance, the coefficient corresponding to surface diffusion type effects, $\mathscr{K} = DR_{eq}\gamma_2 + \phi\alpha_0\alpha_4 - \alpha_0\alpha_2[(1-\phi)D\gamma_0^{-1} - \phi R_{eq}\gamma_2]$, gets contributions, respectively, of thermal origin, due to high-order description of collision cascades [19], and of a mixed nature that is ion-induced (proportional to α_0) but mediated by surface transport (e.g. proportional to D). As discussed elsewhere, Eq. (8) does moreover lead to short range order of the nanodots and intermediate coarsening properties, to the extent that it compares quite favorably not only qualitatively [36], but even *quantitatively* to experiments on e.g. Si targets [37]. The anisotropic version of this equation reads [35]

$$\begin{aligned}\partial_t h = {} & \gamma\partial_x h \\ & + \sum_{i=x,y}\left\{-\nu_i\partial_i^2 h + \lambda_i^{(1)}(\partial_i h)^2 + \Omega_i\partial_i^2\partial_x h + \xi_i(\partial_x h)(\partial_i^2 h)\right\} \\ & + \sum_{i,j=x,y}\left\{-\mathscr{K}_{ij}\partial_i^2\partial_j^2 h + \lambda_{ij}^{(2)}\partial_i^2(\partial_j h)^2\right\}, \end{aligned} \quad (9)$$

where again coefficients are functions of physical parameters, also leading to non-uniform ripple transport and coarsening, and to good qualitative comparison with some experiments (see e.g. in [6,13]). Hence, up to 2008 an improved continuum description had been achieved[1] that indeed generalizes previous descriptions in the intended way. Thus, this "hydrodynamic" formulation is versatile enough to incorporate previous theories such as BH in order to relate microscopic mechanisms with model parameters, while being able to separate the essential mechanisms involved in the formation of the pattern. In general, nonuniform pattern dynamics is predicted that can be roughly broken down into various time regimes including a pattern formation (morphological instability) transient, followed by coarsening/transport and ordering, then large scale roughening, and finally reaching the stationary state. The time extent of each regime depends on system parameters through the coefficients in the appropriate equation of motion.

4. Some caveats

Although the two-field model discussed in the previous section can account for a large number of experimental properties of IBS surface nanopatterns, a number of issues still seem to require a deeper reflection on the basics of this pattern formation process from a general point of view. We can mention some of these issues that have become increasingly relevant in recent years, such as (i) special properties of order and coarsening; (ii) the role of impurities and/or preferential sputtering, and the related (iii) lack of pattern formation at small angles of incidence in some pure monoelemental targets; (iv) by construction the model is *local*, namely, it cannot account for long range interactions.

[1] For an alternative two-field formulation, see [38].

4.1. Long range order/issues on coarsening

As mentioned in the previous section, in general the "hydrodynamic" model just discussed leads to the expectation of a coarsening transient right after the exponential regime induced by the morphological instability dies out. The duration of such an intermediate coarsening period would depend on experimental conditions, but in any case it would be followed either by another period dominated by surface kinetic roughening, or else by saturation to the stationary state [39]. In this sense, there are experimental observations that do not agree with such an expectation. For instance, under 1.2 keV Kr^+ irradiation of Si, highly long-range ordered ripples are produced [40] (in contrast with the short-range order associated with the model of Section 3), that do not show any coarsening. Although the long time, large scale behavior of these morphologies suggests some onset of long wavelength corrugations, it seems hard to reconcile these structures with those predicted e.g. by Eq. (9). Likewise, the coarsening properties of Si targets irradiated by Ar^+ at 500 eV [41] seem to evade those expected for the latter equation: in these experiments, coarsening of the ripple wavelength continues even after saturation of the surface roughness, that again is unexpected for the "hydrodynamic" model.

4.2. Role of impurities and/or preferential sputtering

An important observation was reported in [42] for Si bombardment with 1 keV Ar^+, that "seeding" was required in their experiments in order to induce nanodot formation, that was not achieved for clean samples. After this, an increasing awareness has aroused in the community that intentional or accidental contamination with metallic species is needed in order to trigger the pattern formation process in some pure monoelemental targets. In more recent times, interesting consequences have been derived from this fact, as it seems that the concentration and type of impurities can be tuned in order to control the type of morphology (holes, dots, ripples, etc.) that develops [43–45]. At any rate, this property might be related with the role that preferential sputtering is hypothesized [46] to have in the morphological instability, although more systematic theoretical and experimental studies seem to be required.

4.3. Lack of pattern formation at small incidence angles

The observation by Ozaydin et al. on the lack of pattern formation for the case of clean targets was made for normal incidence conditions. Actually, similar observations had been reported much earlier [47], although at that time no connection to the possible role of (the lack of) impurities had been made; more recent confirmations are also available, see e.g. [41]. Working also with Si targets at a higher energy (10–40 keV), Carter and Vishnyakov [47] attributed, rather, their pattern-less surfaces to a process by which, due to momentum transfer, the ion beam would induce down-hill currents on the surface that would tend to smooth out surface features for small incidence angles. Due to the difficulty in the parametrization of this effect, that had been invoked for a particular experiment, their observation remained relatively unconnected from further developments in the modeling of IBS nanopatterns. Further credit for the idea came from studies of ultrasmooth surfaces of amorphous carbon (a-C) films [48]. Although the average ion energy in the MD simulations reported in this reference is at the lower limit of the region we are considering here, suggestive numerical evidence was indeed provided on the net downhill displacement of the target atoms as induced by the ion beam. This property was then employed to argue in favor of the remarkable smoothing dynamics seen on the a-C films analyzed.

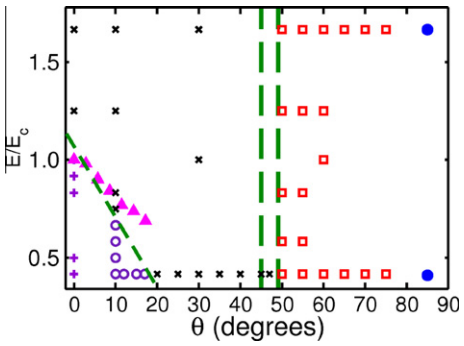

Fig. 2. Adapted from Ref. [50] (E_c = 600 eV). Experimental morphological diagram for Ar^+ IBS of Si. Red squares and blue bullets: ripple formation; black times: flat surfaces; empty purple circles: ripple formation; purple crosses: hole formation. The dashed green lines denote phase boundaries for a type II phase transition (experimental at $\theta_c^{exp} = 48^\circ$ [50] and theoretical at $\theta_c^{theo} = 45^\circ$ [51]) and for a type I transition (oblique line). The theoretical prediction for the latter appears as pink triangles [51]. (For interpretation of the references to colour in this figure legend, the reader is referred to the web version of this article.)

5. Recent data on the morphological instability

In view of the relatively confusing situation[2] in which different (sometimes conflicting) observations were reported under similar conditions, recently a number of experiments have been addressed at clarifying the situation. These works [50] focus on Si targets as a representative case of materials that become amorphous under irradiation, explicitly avoiding metallic impurities. To our knowledge, these are the most complete studies of this type that have been reported to date, hence we will consider them in some detail. Results are summarized in Fig. 2, adapted from this reference. The authors investigate the pattern forming properties of the system using as control parameters the incidence angle and the average ion energy, E. The main features of their results are [50]: (i) no pattern forms for angles below $\theta_c^{exp} = 48^\circ$, this angle value being energy independent; (ii) the morphological transition at θ_c^{exp} is characterized by a wavelength that diverges as $\ell_0 \sim (\theta - \theta_c)^{-1/2}$ for $\theta \gtrsim \theta_c^{exp}$; (iii) there is another transition line at relatively small angles and energies, however, the characteristic pattern wavelength remains constant when approaching this line, and is simply not defined on the side of it corresponding to flat surfaces.

These experimental results pose several difficulties to previous models of IBS nanopatterning [29,50]. On the one hand, the lack of pattern formation for moderate energies is not compatible with BH-type expansions, and cannot be accounted for even by refinement of these through two-field formulations, unless additional relaxation mechanisms are invoked which in principle can be done, see [30,35]. The morphological transition at the energy independent $\theta_c^{exp} = 48^\circ$ line is of type II in the Pattern Formation terminology [21], associated nonetheless with BH-type models. Such transitions are akin to second order or continuous phase transitions in equilibrium Statistical Physics, in which the characteristic length scale in the system diverges at the transition line (equivalently, the associated wave-vector vanishes continuously). On the other hand, the oblique transition line at small (θ, E) seems fundamentally new in this context, being of the so-called type I [21], akin to a first order phase transition. In these transitions, the characteristic wave-vector jumps discontinuously from a finite value (in the pattern forming region) to zero in the flat region. Such type of transition is new in the IBS context, even thinking of additional mechanisms such as e.g. Carter's momentum transfer. Working within a long-wavelength approximation, this led the authors of [29,50] to concluding the relevance of non-local effects that could accommodate such type of behavior, although without sufficient support for specific candidates.

6. Fully hydrodynamical model

In face of the new experimental data discussed in the previous Section, some of us [51] have very recently reconsidered the basic ingredients that are required in the continuum description of IBS surface nanopatterns in order to account within a single framework for, at least, the most salient features of the recent experimental picture of the process. In order to do this, and in view of the large predictive power that ensues when considering the dynamics of material transport, as seen in Section 3, a natural choice is to focus on this process and leave the surface dynamics to arise, rather, as a byproduct of the physical phenomena that are thus taking place in the target. Hence, we focus on the dynamics of the amorphous layer that rapidly builds up and stabilizes in mechanical properties, as described in Section 3. However, we resort to a properly hydrodynamical description that applies to a layer of arbitrary thickness through the study of the appropriate Navier–Stokes equations. In principle, this description should retrieve results for thin layers so that connection with two-field "hydrodynamic" models is expected to be feasible in appropriate parameter ranges. Actually, previous experimental [52] and theoretical [10,53] approaches to the IBS problem through the effects of viscous flow are available, although no general description of the process had been thus achieved so far.

Note that any fully hydrodynamical approach to this system has to rely on the fact that the present type of material flow is highly viscous (viscosity of the amorphized layer is in the 10^8 Pa · s range [54]), so that actually Stokes flow applies. After this, we need to specify the remaining conservation and constitutive laws that apply to our system. Thus, we take the flowing layer to be Newtonian and incompressible, and of a stationary thickness h (see Fig. 3), which is achieved by setting the erosion rate at the free interface to equal the erosion rate at the amorphous/crystalline (a/c) interface. The effect of the ion beam is incorporated as a body force acting in the bulk of the fluid that takes into account the reduction of the ion flux due to non-zero values of the local slope of the free surface. Hence, this mechanism is reminiscent of Carter's [47], but crucially not restricted to act *along* the surface but being present, rather, in the *bulk* of the flowing layer. The coefficient f_E mediating this mechanism has units of a stress gradient, and its value can be inferred [51] from experiments [50] and MD simulations [55], an order of magnitude estimate that agrees with morphological data being 0.42 kg nm^{-2} s^{-2}. Finally, as for the boundary conditions in

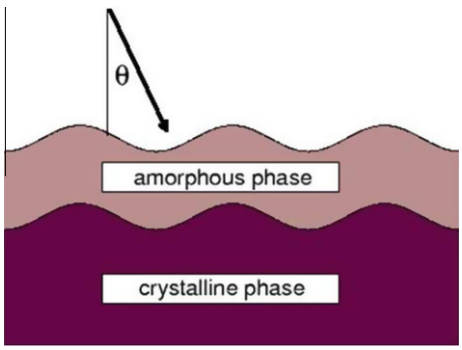

Fig. 3. Schematic view of an IBS experiment. An amorphous layer of thickness h flows as a highly viscous fluid on top of a crystalline substrate.

[2] For a faithful view on the status of our understanding of IBS nanopatterns only one year ago, see [49] and other papers in the same special issue.

our flow model, there is no externally imposed stress, while surface tension is assumed to act at the free interface, and a no-slip condition is taken at the a/c interface.

As mentioned above, this fluid dynamics has an effect on the shape of the free boundary. In order to assess this, one typically considers an initially flat interface and assesses its stability with respect to periodic modulation of wave-vector k, finding that perturbations evolve with an amplitude proportional to $\exp(\omega_k t)$, where [51]

$$\Re e\omega_k = -\frac{\left(f_E\cos 2\theta + k^2\gamma\right)(-2hk+\sinh 2hk)}{2k\mu\left(1+2h^2k^2+\cosh 2hk\right)} + \Re e\overline{\omega}_k. \tag{10}$$

Here, μ is the ion-induced viscosity and $\overline{\omega}_k$ is the contribution to this so-called dispersion relation, due to purely erosive mechanisms akin to Γ_{ex} in Eq. (6). Eq. (10) shows that, in this hydrodynamic formulation, ion-driving and material relaxation couple in a natural albeit non-trivial way that generalizes known results. We should emphasize that the specific form of the dispersion relation, $\Re e\omega_k$, is not essential in order to understand its significance. Thus, note that it can be written in the form

$$\Re e\omega_k = -\frac{f_E\cos 2\theta + k^2\gamma}{2k\mu}F(hk), \tag{11}$$

with $F(\cdot)$ being a single variable function. This means that, even in the limit in which the pattern wavelength is much larger than the thickness of the amorphous layer, nonlocal effects—reflected in the overall prefactor in Eq. (11)— may be responsible for the type I phase transition.

Eq. (10) provides valuable qualitative information about the role of the different parameters that appear. Thus, in the absence of the beam ($f_E = 0$), Eq. (10) reduces to the classic result by Orchard [56] on the rate of smoothing for the free surface of a fluid layer of arbitrary thickness. Actually, the thin-layer limit of the latter was employed by Umbach *et al.* as mentioned in Section 3, while the thick-layer limit leads to Mullins' [16] rate of surface relaxation by bulk viscous flow, employed in [52] to account for experimental results on smoothing of silica targets. Further detailed analysis of Eq. (10) leads to the following conclusions [51]:

1. By neglecting the erosive contribution $\overline{\omega}_k$, Eq. (10) predicts a type II morphological transition at an energy independent angle $\theta_c^{\text{theo}} = 45^\circ$, see Fig. 2, and with the same features as in the experiment, in the sense that flat surfaces occur for $\theta < \theta_c^{\text{theo}}$ while pattern formation takes place for $\theta > \theta_c^{\text{theo}}$. The value 1/2 derived from (10) for the exponent of the divergence of the typical wavelength at θ_c^{theo} and other details of the transition [51], also agree with experimental measurements.
2. Taking for definiteness expressions derived within BH's approach for the purely erosive growth rate $\overline{\omega}_k$, the ensuing energy dependence makes it compete with the additional flow-type contributions to (10), once an energy dependence is assumed also for the latter [57]. As a result, a type I transition takes place along a line in (θ, E) parameter space, that is shown by pink triangles in Fig. 2.

Although still many details need to be improved, the simultaneous occurrence of both types of transitions and the good agreement with experiments, especially in the case of the type II transition, lend credit to the hydrodynamic description put forward in [51]. But note that in this case a substantial change is introduced in our physical understanding on the nature of the morphological instability. Thus, rather than being purely "erosive" as in BH's picture of a curvature dependent sputtering yield, the instability sets in as a result of the different exposure to the the ion beam of the different regions in the amorphous layer.[3] These differences imply facilitated flow for regions that are more directly exposed to the beam, while flow is relatively hampered in regions that receive a reduced flux. For incidence angles above the threshold value θ_c^{theo}, incompressibility of the layer makes the fluid "bulge" out, leading to pattern formation. An analogy with fluid flow down an inclined plane for a non-homogeneous gravity field [51] can provide an intuitive physical picture of the phenomenon. Pursuing this image further, and given the slow speeds that are typical of the present case and the fact that flow itself is eventually due to defect generation and dynamics, flow of a glacier may provide a better macroscopic analog for IBS nanopatterning than the evolution of a sand dune. Coming back to IBS systems, we expect this hydrodynamical description to apply quite generically. For instance, a similar behavior would be presumed for other materials than crystalline Si targets (such as amorphous Si, glass, or amorphous silica) where a thin material layer is expected to flow, driven by the ion beam, on top of an amorphous immobile bulk. As a consequence, in these systems the BH-type morphological instability might also be absent for a range of incidence angles.

7. Conclusions and outlook

As a general conclusion, we believe that continuum models still hold promise for describing surface nanopatterning under IBS, although, at present, many issues remain quite open. Already working within the scope of Section 6 there are many details, such as the energy dependence of the bulk force or an accurate representation of erosive contributions, that would indeed benefit from complementary approaches, such as more atomistic models, and of course from experimental assessment. At any rate, the attention of further efforts needs to be directed to an understanding of the dynamics of the amorphous layer. Naturally, additional features need to be incorporated and understood, such as the anisotropy of the IBS setup and its relevance for transitions among different patterns. Also, as suggested by the model in Ref. [51], a full understanding of the *stress* field beneath the surface seems a candidate for new and exciting research in the upcoming years, both for theoreticians and experimentalists. Once the role of impurities and preferential sputtering is incorporated, a full picture of the IBS nanopatterning process can be envisaged to arise that finally leads to a complete harnessing of this fascinating *bottom-up* route to self-organized surface nanostructuring.

Acknowledgments

This work has been partially supported by the Spanish Ministry of Science and Innovation (Grants Nos. FIS2009-12964-C05-01, FIS2009-12964-C05-03, FIS2009-12964-C05-04, and CSD2008-00023).

References

[1] R.L. Cunningham, P. Haymann, C. Lecomte, W.J. Moore, J.J. Trillat, J. Appl. Phys. 31 (1960) 839.
[2] M. Navez, C. Sella, D. Chaperot, C. R. Acad. Sci. Paris 254 (1962) 240.
[3] H. Gnaser, Low Energy Ion Irradiation of Solid Surfaces, Springer, New York, 1998.
[4] F. Buatier de Mongeot, U. Valbusa, J. Phys. Condens. Matter 21 (2009) 224022.
[5] W.L. Chan, E. Chason, J. Appl. Phys. 101 (2007) 121301.
[6] J. Muñoz-García, L. Vázquez, R. Cuerno, José A. Sánchez-García, M. Castro, R. Gago, in: Z.M. Wang (Ed.), Towards Functional Nanomaterials, Springer, New York, 2009.
[7] S. Facsko, T. Dekorsy, C. Koerdt, C. Trappe, H. Kurz, A. Vogt, H.L. Hartnagel, Science 285 (1999) 1551.

[3] In this sense, flow effects can provide the non-local mechanisms speculated upon earlier [29,50].

[8] B. Ziberi, F. Frost, M. Tartz, H. Neumann, B. Rauschenbach, Appl. Phys. Lett. 92 (2008) 063102.
[9] S. Habenicht, K.P. Lieb, J. Koch, A.D. Wieck, Phys. Rev. B 65 (2002) 115327.
[10] P.F.A. Alkemade, Phys. Rev. Lett. 96 (2006) 107602.
[11] B. Andreotti, P. Claudin, O. Pouliquen, Phys. Rev. Lett. 96 (2006) 028001.
[12] D.D. Vvedensky, J. Phys. Condens. Matter 16 (2004) R1537.
[13] R. Cuerno, M. Castro, J. Muñoz-García, R. Gago, L. Vázquez, Eur. Phys. J. Special Topics 146 (2007) 427.
[14] R.M. Bradley, J.M.E. Harper, J. Vac. Sci. Technol. A 6 (1988) 2390.
[15] P. Sigmund, Phys. Rev. 184 (1969) 383;
J. Mat. Sci. 8 (1973) 1545.
[16] W.W. Mullins, J. Appl. Phys. 28 (1957) 333.
[17] R. Ditchfield, E.G. Seebauer, Phys. Rev. B 63 (2001) 125317.
[18] R. Cuerno, A.-L. Barabási, Phys. Rev. Lett. 74 (1995) 4746.
[19] M.A. Makeev, A.-L. Barabási, Appl. Phys. Lett. 71 (1997) 2800.
[20] M.A. Makeev, R. Cuerno, A.-L. Barabási, Nucl. Instrum. Meth. Phys. Res. B 97 (2002) 185.
[21] M. Cross, H. Greenside, Pattern Formation and Dynamics in Nonequilibrium Systems, Cambridge University Press, Cambridge, England, 2009.
[22] A.-L. Barabási, H.E. Stanley, Fractal Concepts in Surface Growth, Cambridge University Press, Cambridge, England, 1995.
[23] S. Habenicht, W. Bolse, K.P. Lieb, K. Reimann, U. Geyer, Phys. Rev. B 60 (1999) R2200.
[24] S. Facsko, T. Bobek, A. Stahl, H. Kurz, T. Dekorsy, Phys. Rev. B 69 (2004) 153412.
[25] T.C. Kim et al., Phys. Rev. Lett. 92 (2004) 246104.
[26] M. Castro, R. Cuerno, Phys. Rev. Lett. 94 (2005) 139601.
[27] T.C. Kim et al., Phys. Rev. Lett. 94 (2005) 139602.
[28] M. Feix, A.K. Hartmann, R. Kree, J. Muñoz-García, R. Cuerno, Phys. Rev. B 71 (2005) 125407.
[29] B. Davidovitch, M.J. Aziz, M.P. Brenner, Phys. Rev. B 76 (2007) 205420;
J. Phys. Condens. Matter 21 (2009) 224019.
[30] T. Aste, U. Valbusa, Physica A 332 (2004) 548;
New J. Phys. 7 (2005) 122.
[31] Z. Csahók, C. Misbah, F. Rioual, A. Valance, Eur. Phys. J. E 3 (2000) 71.
[32] M.C. Moore, N. Kalyanasundaram, J.B. Freund, H.T. Johnson, Nucl. Instrum. Methods Phys. Res. B 225 (2004) 241.
[33] C.C. Umbach, R.L. Headrick, K. Chang, Phys. Rev. Lett. 87 (2001) 246104.
[34] M. Castro, R. Cuerno, L. Vázquez, R. Gago, Phys. Rev. Lett. 94 (2005) 016102;
J. Muñoz-García, R. Cuerno, M. Castro, J. Phys. Condens. Matter 21 (2009) 224020.
[35] J. Muñoz-García, M. Castro, R. Cuerno, Phys. Rev. Lett. 96 (2006) 086101;
J. Muñoz-García, R. Cuerno, M. Castro, Phys. Rev. B 78 (2008) 205408.
[36] R. Gago, L. Vázquez, O. Plantevin, T.H. Metzger, J. Muñoz-García, R. Cuerno, M. Castro, Appl. Phys. Lett. 89 (2006) 233101.
[37] J. Muñoz-García, R. Gago, L. Vázquez, J.A. Sánchez-García, R. Cuerno, Phys. Rev. Lett. 104 (2010) 026101.
[38] R. Kree, T. Yasseri, A.-K. Hartmann, Nucl. Instrum. Methods Phys. Res. B 267 (2009) 1403.
[39] J. Muñoz-García, R. Cuerno, M. Castro, Phys. Rev. E 74 (2006) 050103(R).
[40] F. Frost, B. Ziberi, A. Schindler, B. Rauschenbach, Appl. Phys. A 91 (2008) 551.
[41] A. Keller, S. Roßbach, S. Facsko, W. Möller, Nanotechnology 19 (2008) 135303.
[42] G. Ozaydin, A.S. Özcan, Y. Wang, K.F. Ludwig, H. Zhou, R.L. Headrick, D.P. Siddons, Appl. Phys. Lett. 87 (2005) 163104.
[43] H. Hofsäss, K. Zhang, Appl. Phys. A 92 (2008) 157.
[44] J.A. Sánchez-García, L. Vázquez, R. Gago, A. Redondo-Cubero, J.M. Albella, Zs. Czigány, Nanotechnology 19 (2008) 355306.
[45] S. Macko, F. Frost, B. Ziberi, D.F. Förster, Th. Michely, Nanotechnology 21 (2010) 085301.
[46] V.B. Shenoy, W.L. Chan, E. Chason, Phys. Rev. Lett. 98 (2007) 256101.
[47] G. Carter, V. Vishnyakov, Phys. Rev. B 54 (1996) 17647.
[48] M. Moseler, P. Gumbsch, C. Casiraghi, A.C. Ferrari, J. Robertson, Science 309 (2005) 1545.
[49] R. Cuerno, L. Váquez, R. Gago, M. Castro, J. Phys. Condens. Matter 21 (2009) 220301.
[50] C.S. Madi, B. Davidovitch, H.B. George, S.A. Norris, M.P. Brenner, M.J. Aziz, Phys. Rev. Lett. 101 (2008) 246102;
C.S. Madi, H.B. George, M.J. Aziz, J. Phys. Condens. Matter 21 (2009) 224010.
[51] M. Castro, R. Cuerno. <arXiv:1007.2144[cond-mat]>.
[52] E. Chason, T.M. Mayer, B.K. Kellermann, D.E. McIlroy, A.J. Howard, Phys. Rev. Lett. 72 (1994) 3040;
T.M. Mayer, E. Chason, A.J. Howard, J. Appl. Phys. 76 (1994) 1633.
[53] A.S. Rudy, V.K. Smirnov, Nucl. Instrum. Methods Phys. Res. B 159 (1999) 52.
[54] S.G. Mayr, Y. Ashkenazy, K. Albe, R.S. Averback, Phys. Rev. Lett. 90 (2003) 055505.
[55] N. Kalyanasundaram, M. Wood, J.B. Freund, H.T. Johnson, Mech. Res. Comm. 35 (2008) 50.
[56] S.E. Orchard, Appl. Sci. Res. 11A (1962) 451.
[57] C.A. Davis, Thin Solid Films 226 (1993) 30.